

# Analytic perturbation theory: A new approach to the analytic continuation of the strong coupling constant $\alpha_s$ into the timelike region

Kimball A. Milton\*

*Department of Physics and Astronomy, The University of Oklahoma, Norman, Oklahoma 73019*

Olga P. Solovtsova†

*Bogoliubov Laboratory of Theoretical Physics, Joint Institute for Nuclear Research, Dubna, Moscow Region, 141980, Russia*

(Received 14 October 1997; published 3 April 1998)

The renormalization group applied to perturbation theory is ordinarily used to define the running coupling constant in the spacelike region. However, to describe processes with timelike momenta transfers, it is important to have a self-consistent determination of the running coupling constant in the timelike region. The technique called analytic perturbation theory (APT) allows a consistent determination of this running coupling constant. The results are found to disagree significantly with those obtained in the standard perturbative approach. Comparison between the standard approach and APT is carried out to two loops, and threshold matching in APT is applied in the timelike region.

[S0556-2821(98)00411-1]

PACS number(s): 11.10.Hi, 11.55.Fv, 12.38.Cy, 13.35.Dx

## I. INTRODUCTION

A fundamental issue in quantum chromodynamics (QCD) is the behavior of the strong interaction running coupling constant  $\alpha_s = g_s^2/4\pi$ . The basic research tool is perturbation theory (PT) with its renormalization-group improvement [1]. In the QCD case in the limit of large momentum transfers  $Q$ , this approach provides a logarithmic decrease of the running coupling constant  $\alpha_s \sim 1/\ln(Q^2/\Lambda^2)$ , where  $\Lambda$  is the QCD scale parameter that determines where the theory becomes asymptotically free. The study of the behavior of  $\alpha_s$  outside of the asymptotic region is more difficult. It is known that the direct use of PT improved by the renormalization group leads to infrared instability of  $\alpha_s$  and unphysical singularities, for instance, a ghost pole at  $Q^2 = \Lambda^2$ . Unphysical singularities of a perturbative running coupling constant preclude a self-consistent determination of the effective coupling constant for timelike momentum transfers. Recently, a new method has been proposed [2] for constructing the QCD running coupling constant in such a way as to retain the correct analytic properties. This method is called analytic perturbation theory (APT). The main purpose of this paper is to analyze the region of timelike momentum transfers on the basis of APT [2,3], and compare the results of the PT and APT approaches.

It is well known that a theoretical description of important timelike processes such as  $e^+e^-$  annihilation into hadrons, or of decay widths of the  $\tau$ -lepton and  $Z$ -boson into hadrons, requires analytic continuation of the running coupling constant from the spacelike (Euclidean) region of momentum transfers ( $q^2 = -Q^2 < 0$ ) into the timelike (physical) region ( $q^2 > 0$ ). Although this problem has been studied since the 1970s (see, e.g., [4]), it still remains a subject of great inter-

est (see, e.g., [5–7]). It is obvious that information on the running coupling constant obtained from timelike processes, for instance, from  $e^+e^-$  annihilation into hadrons, corresponds to knowledge of the coupling constant extracted from spacelike processes such as deep inelastic scattering, if the transition from the Euclidean into the physical region is performed in a correct manner (see [3,8]) without violation of analytic properties of the hadronic correlator  $\Pi(q^2)$  and the Adler function  $D(q^2)$ . When the analytic properties are not respected, the question arises: To what extent does this breaking of analyticity influence quantities extracted from physical processes? It is impossible to answer this question within the framework of standard perturbation theory. On the other hand, the APT method retains the correct analytic properties of the Adler  $D$ -function and, in addition, gives simple analytic expressions that can be compared with corresponding PT expressions and, therefore, allows quantitative analysis of the influence that the breaking of  $Q^2$ -analyticity has on the running coupling constant.

The organization of this paper is as follows: In the following section, we discuss the procedure of analytic continuation from the spacelike (Euclidean) to the timelike ( $s$ -channel) region. In Sec. III we examine this procedure in the conventional one-loop PT approach, and demonstrate that it is inconsistent. In Sec. IV we resolve this problem through the APT approach, and in Sec. V we compare the results of these two schemes. We move on to two-loops in Sec. VI, and demonstrate the stability of the APT approach. A matching procedure for timelike momentum transfers is given in Sec. VII, where we show how the coupling constant depends on the number of active flavors. A summary of our results is given in the Conclusions.

## II. EFFECTIVE COUPLING CONSTANTS IN THE TIMELIKE AND SPACELIKE REGIONS

First, we note that in the standard approach, the running coupling constant in QCD as a function of  $Q^2$  is determined

\*E-mail address: milton@mail.nhn.ou.edu

†E-mail address: olsol@thsun1.jinr.dubna.su

by the renormalization-group analysis in the region of space-like momentum transfers. However, to parametrize many physical processes, one needs to know the coupling constant in the timelike region. To be specific, many experimentally measured ratios  $R_\sigma$ , where, e.g.,  $\sigma = e^+e^-$ ,  $\tau$ ,  $Z$ , . . . , can be written in the form  $R_\sigma = R_\sigma^{(0)}(1 + \Delta_\sigma)$ . Here  $\Delta_\sigma$  is a QCD correction and  $R_\sigma^{(0)}$  represents the parton level of description of a given process with electroweak corrections.  $\Delta_\sigma$  can be expressed through the imaginary part of the hadronic correlator  $\mathcal{R}(s) = \text{Im} \Pi(s)/\pi$ . To parametrize  $\mathcal{R}(s)$  in terms of QCD parameters, a special procedure of analytic continuation is required. With that end in view, one usually employs a dispersion relation

$$D(z) = -z \frac{d\Pi(z)}{dz} = -z \int_0^\infty ds \frac{\mathcal{R}(s)}{(s-z)^2}, \quad (1)$$

where  $z = q^2$ , and the inverse relation

$$\mathcal{R}(s) = \frac{1}{2\pi i} \int_{s-i\epsilon}^{s+i\epsilon} dz \frac{d\Pi(z)}{dz} = -\frac{1}{2\pi i} \int_{s-i\epsilon}^{s+i\epsilon} dz \frac{D(z)}{z}, \quad (2)$$

where the contour joins points  $s \mp i\epsilon$  and lies in the region of analyticity of the function  $D(z)$ , going around the cut  $\text{Re } z > 0$ .

We define the effective coupling constants  $\bar{a}^{\text{eff}}$  and  $\bar{a}_s^{\text{eff}}$ , respectively, in the spacelike ( $t$ -channel) and timelike ( $s$ -channel) regions, using the notation  $\bar{a} = \bar{a}/4\pi$  and dimensionless (in units of the scaling parameter  $\Lambda$ ) momentum variables, by

$$D(z) \propto 1 + d_1 \bar{a}(z) + d_2 \bar{a}^2(z) + \dots = 1 + d_1 \bar{a}^{\text{eff}}(z), \quad (3)$$

$$\mathcal{R}(s) \propto 1 + r_1 \bar{a}_s(s) + r_2 \bar{a}_s^2(s) + \dots = 1 + r_1 \bar{a}_s^{\text{eff}}(s). \quad (4)$$

Relations (1) and (2) and the equality  $d_1 = r_1$  result in the connection between these effective coupling constants

$$\bar{a}_s^{\text{eff}}(s) = -\frac{1}{2\pi i} \int_{s-i\epsilon}^{s+i\epsilon} \frac{dz}{z} \bar{a}^{\text{eff}}(z), \quad (5)$$

$$\bar{a}^{\text{eff}}(z) = -z \int_0^\infty \frac{ds}{(s-z)^2} \bar{a}_s^{\text{eff}}(s). \quad (6)$$

Therefore, the QCD corrections  $\Delta_\sigma$  for the class of physical processes considered with timelike momentum transfers are to be parametrized, according to Eq. (4), by the effective coupling constant  $\bar{a}_s^{\text{eff}}(s)$ , which is explicitly related to  $\bar{a}^{\text{eff}}(z)$  by Eqs. (5) and (6).

In any finite order of PT, the analytic properties of the running coupling  $\bar{a}(z)$  should be the same as for the effective coupling constant  $\bar{a}^{\text{eff}}(z)$ . Therefore, the connection between  $t$ - and  $s$ -channel running coupling constants,  $\bar{a}(z)$  and  $\bar{a}_s(s)$  is defined by equations like (5) and (6). In the one-loop approximation the effective coupling constants coincide with the running coupling constants and in higher loops, the connection depends on the physical process.

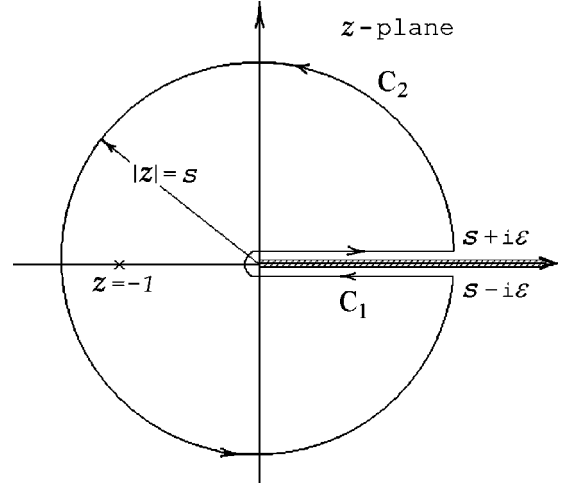


FIG. 1. Integration contours in the complex  $z$ -plane.

### III. PT ANALYSIS

Consider the above procedure of analytic continuation within PT. In the one-loop approximation, the running coupling constant is of the form

$$\bar{a}^{\text{PT}}(z) = \frac{1}{\beta_0} \frac{1}{\ln(Q^2/\Lambda^2)} = \frac{1}{\beta_0} \frac{1}{\ln(-z)}, \quad z \equiv -Q^2/\Lambda^2, \quad (7)$$

where  $\beta_0 = 11 - 2n_f/3$  is the one-loop coefficient of the  $\beta$ -function corresponding to  $n_f$  active quarks. Inserting Eq. (7) into Eq. (5) we obtain the following expression for the running coupling constant in  $s$ -channel:

$$\begin{aligned} \bar{a}_s^{\text{PT}}(s) &= -\frac{1}{2\pi i \beta_0} \int_{s-i\epsilon}^{s+i\epsilon} \frac{dz}{z} \frac{1}{\ln(-z)} \\ &= -\frac{1}{\pi \beta_0} \left( \frac{\pi}{2} + \arctan \frac{\ln s}{\pi} \right). \end{aligned} \quad (8)$$

This expression is physically meaningless, because it is negative for any  $s$  and does not have the correct asymptotics, that is, going as  $1/\ln s$  as  $s \rightarrow \infty$ ; the reason will be explained below.

There is another way of calculating  $\bar{a}_s$ , based on the Shankar method [9]. Using analyticity of the  $D$ -function in the complex  $z$ -plane with the cut along the positive real axis, we may pass from the integral along the cut, given by expression (5), that is, around the contour  $C_1$  (see Fig. 1), to an integral around a circle of radius  $|z|=s$  in the complex  $z$ -plane, contour  $C_2$ , parametrized by  $z = -s \exp(i\varphi)$ ,  $-\pi < \varphi < \pi$ , to arrive at the expression

$$\begin{aligned} \bar{a}_s^{\text{PT}}(s) &= \frac{1}{2\pi i} \int_{C_2} \frac{dz}{z} \bar{a}^{\text{PT}}(z) = \frac{1}{2\pi \beta_0} \int_{-\pi}^{\pi} \frac{d\varphi}{\ln s + i\varphi} \\ &= \frac{1}{\pi \beta_0} \arctan \frac{\pi}{\ln s}; \end{aligned} \quad (9)$$

this is positive when  $s > 1$  and possesses the correct ultraviolet asymptotics. It is just this expression that is used as a one-loop PT result for all timelike momenta  $s > 0$ :

$$\bar{\alpha}_s^{\text{PT}}(s) = \frac{4}{\beta_0} \arctan \frac{\pi}{\ln s}. \quad (10)$$

It is obvious that Eq. (10) provides the restriction  $\bar{\alpha}_s^{\text{PT}}(s) \leq 2\pi/\beta_0$  for any  $s$  (see [10]).

Thus, a formal conversion of the PT one-loop running coupling constant in the spacelike region (7) into expressions for the coupling constant in the timelike region leads to contradictory results (8) and (9). The reason can easily be understood if one applies the Cauchy theorem (see Fig. 1) to establish the connection between the integrals in Eqs. (8) and (9),

$$\frac{1}{2\pi i} \int_{C_2} dz \psi(z) = -\frac{1}{2\pi i} \int_{C_1} dz \psi(z) + \text{res}[\psi(z), -1],$$

$$\psi(z) \equiv \frac{1}{z \ln(-z)}, \quad (11)$$

which is consistent with Eqs. (8) and (9) because the residue of the function  $\psi(z)$  at the point  $z = -1$  is 1. Therefore, the discrepancy between Eq. (8) and Eq. (9) is due to an unphysical ghost pole in Eq. (7) at  $z = -1$  that violates the required analytic properties of the running coupling constant. The inclusion of multiloop corrections does not solve this problem but rather produces new unphysical singularities, as we will see in Sec. VI. Therefore, keeping to standard PT approximations that violate the necessary analytic properties of the running coupling constant makes it impossible to pass into the timelike region in a self-consistent way. This can, for instance, be demonstrated by making an inverse transition from the timelike into the spacelike region with the help of the dispersion relation (1). Substituting the running coupling constant  $\bar{a}_s(s)$  given by Eq. (9) into integral (6) following from Eq. (1) and taking account of the expression  $\arctan(\pi/\ln s) = \text{sgn}(\ln s)\pi/2 - \arctan(\ln s/\pi)$ , we arrive at the formula

$$\bar{a}_s^{\text{PT}}(z) = \frac{1}{\beta_0} \left[ \frac{1}{\ln(-z)} + \frac{1}{1+z} - \frac{1}{1-z} \right], \quad (12)$$

which is different from the starting point, Eq. (7).

#### IV. APT ANALYSIS

The problem of how to make the correct transition between the space- and timelike regions can be solved in the framework of the APT method [2,3] that ensures the correct analytic properties of the coupling constant without introducing extra parameters. The resulting one-loop expression for the analytic coupling constant in the Euclidean region is as follows:

$$\bar{a}_s^{\text{APT}}(z) = \frac{1}{\beta_0} \left[ \frac{1}{\ln(-z)} + \frac{1}{1+z} \right]. \quad (13)$$

The first term in square brackets determines the asymptotic behavior at large momenta and is of the form given in PT. The second term, of a nonperturbative nature, compensates the ghost pole at  $z = -1$ . When one employs the analytic

coupling constant (13), both methods of calculating  $\bar{a}_s$  considered above produce the same result: i.e.,

$$\begin{aligned} \bar{a}_s^{\text{APT}}(s) &= -\frac{1}{2\pi i} \int_{C_1} \frac{dz}{z} \bar{a}^{\text{APT}}(z) = \frac{1}{2\pi i} \int_{C_2} \frac{dz}{z} \bar{a}^{\text{APT}}(z) \\ &= \frac{1}{\pi\beta_0} \left( \frac{\pi}{2} - \arctan \frac{\ln s}{\pi} \right). \end{aligned} \quad (14)$$

We note that APT and PT give distinct values for the running coupling constant in the timelike region: for example,

$$\bar{a}_s^{\text{APT}} = \bar{a}_s^{\text{PT}} + \frac{1}{\beta_0}, \quad (15)$$

where  $\bar{a}_s^{\text{PT}}$  is given by Eq. (8). Consistency of the APT approach also follows from the fact that we can reconstruct the initial expression (13) when the timelike coupling (14) is substituted into Eq. (6). It is of interest to note that this consistency is due to the second term in Eq. (13) that compensates the pole, whose contribution to the integral around the contour  $C_2$  equals zero when  $s > 1$ : i.e., we have the equality

$$\int_{C_2} \frac{dz}{z} \bar{a}^{\text{APT}}(z) = \int_{C_2} \frac{dz}{z} \bar{a}^{\text{PT}}(z), \quad s > 1, \quad (16)$$

where the function  $\bar{a}^{\text{PT}}(z)$  is defined by Eq. (7). Therefore the PT expression (7) gives the same result as the APT approach in the timelike region for  $s > 1$  if the contour  $C_2$  is used. However, there is no inverse correspondence for PT [see formula (12)]. Moreover, note that an equality analogous to Eq. (16) does not arise if the integrand contains the running coupling constant multiplied by a function of  $z$ . For the  $R_\tau$ -ratio, for instance,  $\bar{a}$  is multiplied by a polynomial in  $z$  and, as is shown in [11], the contour integral over  $C_2$  in PT turns out to be different from that in the APT approach.<sup>1</sup>

#### V. NUMERICAL COMPARISON OF RUNNING COUPLING CONSTANTS

The results obtained are illustrated in a series of figures. (In these figures we take the number of quark flavors to be 3.) First, we consider the region of small momentum transfers. Figure 2 shows the behavior of the running coupling constant computed by different methods in the region  $-10 \leq s = q^2/\Lambda^2 \leq 10$ . The solid line represents the APT coupling constant calculated by formula (13) in the spacelike region (number 1 in the figure) and by formula (14) in the time-like region (curve 1\*). Dots denote the ‘‘PT’’ coupling constant determined by Eq. (10) (curve 2\*) and by Eq. (12) (curve 2). The dash-dotted line 3 represents the PT coupling constant computed by formula (7) in the spacelike region, and curve 3\* by formula (8) in the timelike region. (Incidentally, note that curves 2 and 2\* vanish at the origin, which is beyond the resolution of this figure, while curves 1 and 1\* approach the

<sup>1</sup>A detailed comparison of inclusive  $\tau$  decay can be found in Ref. [12].

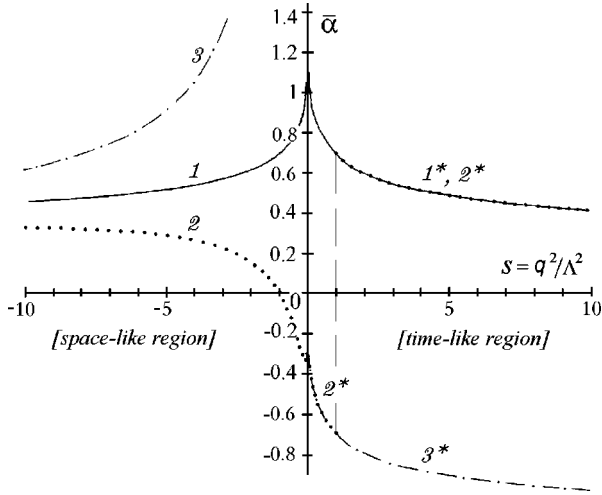


FIG. 2. The behavior of the running coupling constant calculated by different methods as a function of the dimensionless variable  $s = q^2/\Lambda^2$ .

universal value  $4\pi/\beta_0 = 1.40$  at the origin.)

As is seen from Fig. 2, the behavior of the APT running coupling constants (curves 1 and 1\*) is almost, but not quite, mirror-symmetric, and at  $s=0$  the space- and timelike APT running coupling constants are both equal to the universal value  $4\pi/\beta_0$  (see [3]). The pairs of curves of the standard PT approach, 3 and 2\*, or 3 and 3\*, do not show analogous behavior of the running coupling constants. In the spacelike region the function  $\bar{\alpha}^{\text{PT}}$  grows without limit (curve 3), whereas in the timelike region (curve 2\*) it is limited to the value  $2\pi/\beta_0$ . Curve 2 calculated with the coupling given by curve 2\* in the dispersion integral does not reproduce the initial curve 3.

Now consider the region where the running coupling constant  $\bar{\alpha} \sim 0.3$ , which approximately corresponds to the mass scale of the  $\tau$ -lepton,  $M_\tau = 1.78$  GeV,  $\bar{\alpha}(M_\tau) = 0.34 \pm 0.04$  [13], defined in the spacelike region. It is known that the decay  $\tau \rightarrow \text{hadrons}$  is important for testing QCD, as it allows the most accurate determination of the running coupling constant at comparatively low energies (see the review [14]).

Figure 3 shows the behavior of the running coupling constant versus the dimensionless variable  $s = |q^2|/\Lambda^2$ . Notation is the same as in Fig. 2; a dashed horizontal line corresponds to  $\bar{\alpha} = 0.34$ . As it is seen from the Fig. 3, curves 1, 2, 3 that describe the spacelike region noticeably differ from each other. With increasing  $s$ , they begin, as they should, to approach each other, which is demonstrated on the top right of Fig. 3. Values of the parameter  $\Lambda$  calculated with the running coupling constants described by curves 1, 2 and 3 are different. For example, the value of APT-function (curve 1), equal to 0.34 is achieved at  $s_0 = 41.5$ , which corresponds to  $\Lambda^{\text{APT}} = 276$  MeV. For PT-curve 3  $s_0 = 60.5$  and  $\Lambda^{\text{PT}} = 228$  MeV. Note that for curve 2 the value  $\bar{\alpha} = 0.34$  cannot be achieved at any value of  $s$ . For timelike momentum transfers, recall that curves 1\* and 2\* as functions of the dimensionless variable  $s$  coincide when  $s > 1$ . However, they are characterized by different values of  $\Lambda$ , which results in different values of the running coupling constant in the timelike region,  $\bar{\alpha}_s^{\text{APT}}(M_\tau) = 0.31$  and  $\bar{\alpha}_s^{\text{PT}}(M_\tau) = 0.29$ . [The procedure

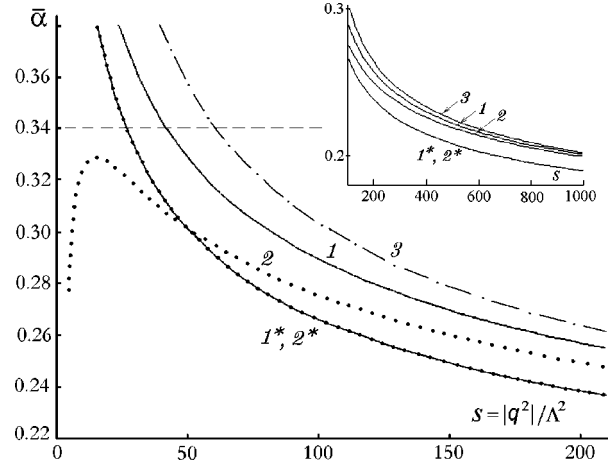


FIG. 3. Behavior of the running coupling constant as a function of the dimensionless variable  $s = |q^2|/\Lambda^2$ . Notation is the same as in Fig. 2; a dashed horizontal line corresponds to  $\bar{\alpha} = 0.34$ . The graph on the right top shows the behavior of the same curves for large values of  $s$ .

here is to use the spacelike value of  $\bar{\alpha}$  to determine  $Q^2/\Lambda^2$ , and then, with the same numerical value of  $s$ , determine  $\bar{\alpha}_s$  from Eq. (14) and Eq. (10), respectively.] With the accuracy attained at present for experimental data on the hadronic decay of the  $\tau$  [14], this quantitative discrepancy is becoming significant.

Let us finally observe the evolution of the running coupling constant in the region of momentum transfers of order of the Z-boson mass  $M_Z = 91.2$  GeV. The running coupling constant  $\bar{\alpha}$ , corresponding to the dimensionless variable  $s$  is drawn in Fig. 4. (At this point, we neglect the change in the number of active quarks with growing energy since this effect does not change the overall picture. We will consider the change in the number of active flavors at the two-loop level in Sec. VII.) The curve denoted by  $\bar{\alpha}$  represents all three curves 1, 2 and 3 that are drawn in Figs. 2 and 3 and describe the behavior of the running coupling constant in the spacelike region, which merge into one curve with high accuracy for these large values of  $s$ . The curve denoted by  $\bar{\alpha}_s$  corresponds to the coupling constant in the timelike region and to

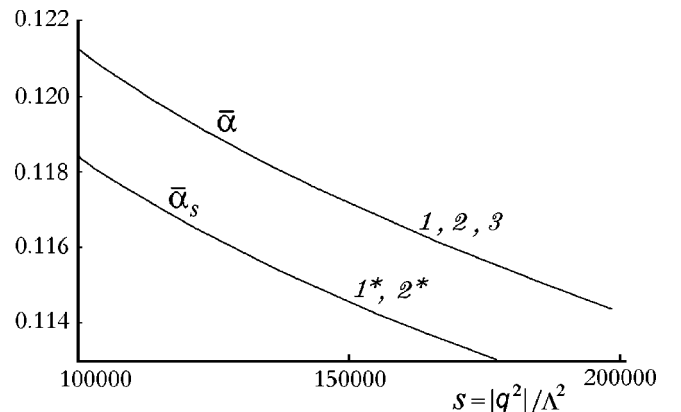


FIG. 4. Behavior of the running coupling constant in the vicinity of the Z-boson mass. Curves 1, 2, 3 and 1\*, 2\* represent the same coupling constants as in Fig. 2 and Fig. 3.

curves  $1^*$  and  $2^*$  plotted in Figs. 2 and 3. In the region of sufficiently large values of  $s$ , the well-known approximate formula with the so-called  $\pi^2$ -term (see, e.g., [7,15])

$$\bar{\alpha}_s = \bar{\alpha} \left( 1 - \frac{\pi^2}{3} \frac{1}{\ln^2 s} \right) \quad (17)$$

works well (with an accuracy  $\sim 0.1\%$ ) both for PT and APT. This approximation gives a difference between  $\bar{\alpha}_s$  and  $\bar{\alpha}$  of about 2%. Substituting the value of the parameter  $\Lambda$  fixed at  $q = M_\tau$ , we obtain the corresponding values of the running coupling constant at  $q = M_Z$ :  $\bar{\alpha}^{\text{APT}} = 0.120$ ,  $\bar{\alpha}^{\text{PT}} = 0.117$  (spacelike region);  $\bar{\alpha}_s^{\text{APT}} = 0.118$ ,  $\bar{\alpha}_s^{\text{PT}} = 0.114$  (timelike region). Thus, even at such large values of  $s$ , the effect of analyticity on the running coupling constant amounts to  $\sim 2\%$ , i.e., it is comparable with the contribution from the  $\pi^2$ -term and from higher PT loop corrections.

## VI. TWO-LOOP RESULTS

We now extend the above considerations to the two-loop level. The distinction between the APT and the PT running coupling constants in the Euclidean region has to do with the unphysical singularities of the PT running coupling constant. Following the results of Ref. [2], we can write down the analytic running coupling constant in the form of a sum of the standard perturbative part and additional terms which

compensate for the contributions of the unphysical singularities, a pole and a cut:

$$\bar{a}^{\text{APT}}(z) = \bar{a}^{\text{PT}}(z) + \Delta \bar{a}_{\text{pole}}(z) + \Delta \bar{a}_{\text{cut}}(z). \quad (18)$$

For the two-loop perturbative running coupling constant, we use [2,12]

$$\bar{a}^{\text{PT}}(z) = \frac{1}{\beta_0} \frac{1}{L + B_1 \ln(1 + L/B_1)}, \quad L = \ln(-z) = \ln \frac{Q^2}{\Lambda^2}, \quad (19)$$

where  $B_1 = \beta_1/\beta_0^2$ , and  $\beta_1 = 102 - 38n_f/3$  is the two-loop coefficient of the  $\beta$ -function. Obviously, at large  $L$  Eq. (19) gives the standard PT expression as an expansion in inverse powers of  $L$ ,

$$\bar{\alpha}_{\text{asymp}}^{\text{PT}} = \frac{4\pi}{\beta_0 L} \left( 1 - B_1 \frac{\ln L}{L} \right) + O\left(\frac{1}{L^3}\right). \quad (20)$$

According to Eq. (19), the contribution coming from the unphysical pole is cancelled by

$$\Delta \bar{a}_{\text{pole}}(z) = \frac{1}{2\beta_0} \frac{1}{1+z}, \quad (21)$$

while the unphysical cut is removed by the following compensation term:

$$\Delta \bar{a}_{\text{cut}}(z) = \frac{1}{\pi\beta_0} \int_0^{\exp(-B_1)} \frac{d\sigma}{\sigma+z} \frac{\pi B_1}{[\ln \sigma + B_1 \ln(-1 - \ln \sigma/B_1)]^2 + \pi^2 B_1^2}. \quad (22)$$

To calculate the analytic running coupling constant in the timelike region, we use the expression in terms of the spectral density  $\varrho(\sigma)$  [3]:

$$\bar{a}_s^{\text{APT}}(s) = \frac{1}{\pi} \int_s^\infty \frac{d\sigma}{\sigma} \varrho(\sigma), \quad (23)$$

where  $\varrho(\sigma) = \text{Im} \bar{a}^{\text{PT}}(-\sigma - i\epsilon)$ . The spectral density  $\varrho$  plays a central role in the APT method; the spacelike running coupling constant,  $\bar{a}^{\text{APT}}$ , is also expressed through  $\varrho$  as follows:

$$\bar{a}^{\text{APT}}(z) = \frac{1}{\pi} \int_0^\infty \frac{d\sigma}{\sigma - z - i\epsilon} \varrho(\sigma). \quad (24)$$

As outlined above, independently of the order of approximation, the APT running coupling constants defined in the space- and timelike regions at  $Q^2=0$  and  $s=0$  are both equal to the universal infrared limiting value  $4\pi/\beta_0$  [3], which is important to establish the stability in the region of the small momentum transfers. (This result is proved in [12].) Consider the region in which the value of running coupling constant  $\bar{\alpha} \sim 0.35$  (the  $\tau$  lepton scale). Figure 5 shows the behavior of the two-loop running coupling constant for the same interval of the dimensionless variable  $s$  as

in Fig. 3. The solid line represents the APT coupling constant in the spacelike region, which can be computed from (18); this is like  $1$  in Figs. 2 and 3. The dotted line denotes the APT coupling constant in the timelike region, computed from (23); this is like  $1^*$  in one-loop. The dashed line rep-

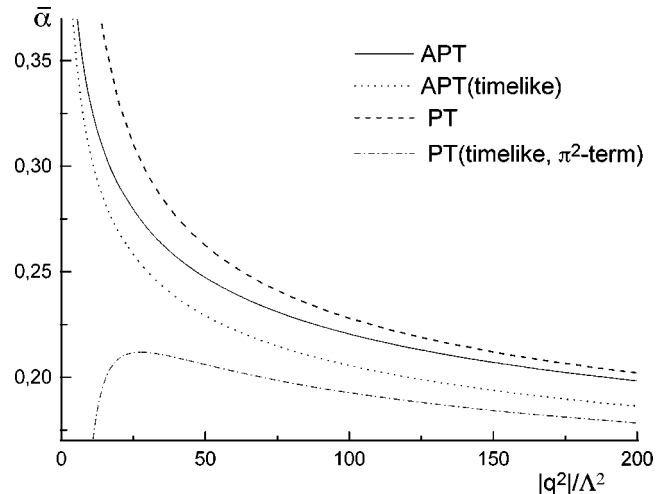


FIG. 5. Behavior of the two-loop running coupling constant in the PT and APT schemes, both in terms of spacelike and timelike definitions.

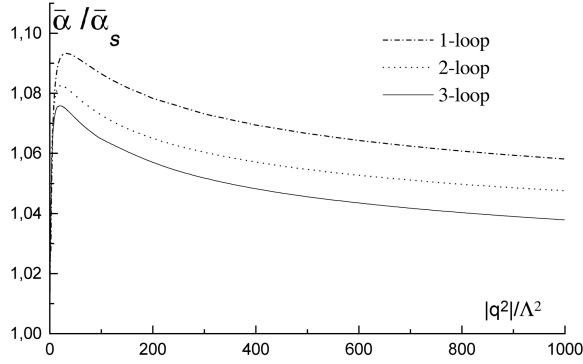


FIG. 6. The ratio of spacelike and timelike values of the running coupling constant in the APT scheme, at one, two, and three loops.

resents the spacelike PT coupling constant defined by formula (19), which is like 3. The dash-dotted curve corresponds to timelike PT coupling constant constructed taking into account  $\pi^2$ -terms, like Eq. (17), and analogous to 2\*. This figure demonstrates that, as in the one-loop case, there is a difference in behavior of all these constants. Moreover, the region in which the value of running coupling constant is about 0.34, is shifted to smaller  $s$ ; the value of 0.34 for the APT running coupling constant is achieved at  $s_0 = 8.6$  which corresponds to  $\Lambda^{\text{APT}} = 607$  MeV and the value of the timelike running coupling constant  $\bar{\alpha}_s^{\text{APT}} = 0.32$ . For the PT running coupling constant,  $s_0 = 18$  and  $\Lambda^{\text{PT}} = 419$  MeV. Thus, while in the one-loop case APT parameter  $\Lambda$ , is 20% larger than PT value, in the two-loop case this discrepancy increases to 45%.<sup>2</sup>

In Fig. 6 we show the stability of APT result for the ratio of the space- and timelike APT running coupling constants. The solid line corresponds to three-loop case, the dashed line is two-loop, and the dot-dash is one-loop. (The one-loop result was already given in [3].)

Let us now demonstrate that in the two-loop approximation, as in the one-loop case, the equality (16) is valid as well. By using Eq. (18), we get

$$2\pi i \bar{a}_s^{\text{APT}} = \int_{C_2} \frac{dz}{z} \bar{a}^{\text{APT}}(z) = \int_{C_2} \frac{dz}{z} \bar{a}^{\text{PT}}(z) + \int_{C_2} \frac{dz}{z} \Delta \bar{a}_{\text{pole}}(z) + \int_{C_2} \frac{dz}{z} \Delta \bar{a}_{\text{cut}}(z). \quad (25)$$

As follows from (21), the pole term has the same structure as in the one-loop approximation, and its contribution to contour integral equals zero when  $s > 1$ . One can also find that the contribution of the cut term (22) in Eq. (25) equals zero when  $s > \exp(-B_1)$ .<sup>3</sup> As a result, the equality (16) holds for  $s > 1$  as well, but it should be stressed (see above discussion in Sec. V) that this does not mean that the APT and PT timelike coupling constants coincide with each other.

<sup>2</sup>In Fig. 5 we do not plot the three-loop result (see [2]), because it practically coincides with the two-loop one.

<sup>3</sup>For  $0 \leq n_f \leq 6$  we have  $0.4 < \exp(-B_1) < 0.6$ .

## VII. $s$ -CHANNEL MATCHING

Let us now discuss the issue of how the parameter  $\Lambda$  changes with energy as the number of active quark changes:  $\Lambda \rightarrow \Lambda_{n_f}$  (see [16] for further details). The relationship between  $\Lambda_{n_f}$  and  $\Lambda_{n_f+1}$  may be fixed by the matching conditions for coupling constant at ‘‘quark thresholds’’ (see, e.g., [17]) which is usually applied to the running coupling constant in the Euclidean region. The APT method opens the new possibility of performing the threshold matching in the physical region, where the number of active quarks can be associated with the energy threshold of quark pair production. It is important to note that any matching procedure of the coupling constant in the Euclidean region, for which one uses the condition of the type  $\text{Re } Q^2 > \xi^2 M_q^2$  (usually  $1 \leq \xi \leq 2$ ), leads to a violation of analyticity of  $\bar{a}(z)$ . Although  $s$ -channel matching demands only continuity of the function  $\bar{a}_s(s)$  at the threshold, and not of its derivatives, the spacelike running coupling constant  $\bar{a}(z)$  will be an analytic function of  $z$ , and due to the representation (6)  $\bar{a}(z)$  ‘‘knows,’’ in principle, about all quark thresholds. Therefore, the APT method gives a more consistent definition of the running coupling constant and a natural way to perform the matching procedure. Within the APT approach, we will require that the timelike function  $\bar{a}_s^{\text{APT}}(s)$  should be a continuous function at the threshold points:

$$\bar{a}_s^{\text{APT}}[(Q_{n_f+1}/\Lambda_{n_f})^2, n_f] = \bar{a}_s^{\text{APT}}[(Q_{n_f+1}/\Lambda_{n_f+1})^2, n_f + 1], \quad (26)$$

where  $Q_{n_f}$  is defined by the pole masses  $M_q$  of quark pair. Taking into account Eqs. (16) and the results of the previous section that the unphysical singularities do not contribute at  $s > 1$  to the contour integral we can rewrite Eq. (26) in the following form:

$$\int_{|z|=(Q_{n_f+1}/\Lambda_{n_f})^2} \frac{dz}{z} \bar{a}^{\text{PT}}(z, n_f) = \int_{|z|=(Q_{n_f+1}/\Lambda_{n_f+1})^2} \frac{dz}{z} \bar{a}^{\text{PT}}(z, n_f + 1). \quad (27)$$

Therefore, the conventional matching condition

$$\bar{a}^{\text{PT}}[(Q_{n_f+1}/\Lambda_{n_f})^2, n_f] = \bar{a}^{\text{PT}}[(Q_{n_f+1}/\Lambda_{n_f+1})^2, n_f + 1], \quad (28)$$

which one usually uses in perturbation theory, is modified and written down as the relation of the contour integrals, Eq. (27).

As an example, consider a change of the two-loop scale parameter  $\Lambda$  when passing through a quark pair threshold in PT and APT by using  $\alpha(M_c) = 0.34$  and the following values of pole  $c$ -,  $b$ - and  $t$ -quark masses  $M_c = 1.6$  GeV,  $M_b = 4.5$  GeV, and  $M_t = 174$  GeV and  $Q_4 = 2M_c$ ,  $Q_5 = 2M_b$ ,  $Q_6 = 2M_t$ . In the perturbative case, we find  $\Lambda_3^{\text{PT}} = 419$  MeV,  $\Lambda_4^{\text{PT}} = 338$  MeV,  $\Lambda_5^{\text{PT}} = 230$  MeV, and  $\Lambda_6^{\text{PT}} = 92.6$  MeV, the ratios of which obey the well-known relations from Ref. [17]. In the APT case, we obtain  $\Lambda_3^{\text{APT}} = 607$  MeV,  $\Lambda_4^{\text{APT}} = 471$  MeV,  $\Lambda_5^{\text{APT}} = 316$  MeV, and  $\Lambda_6^{\text{APT}} = 129$  MeV. The ratios of these quantities are close to the

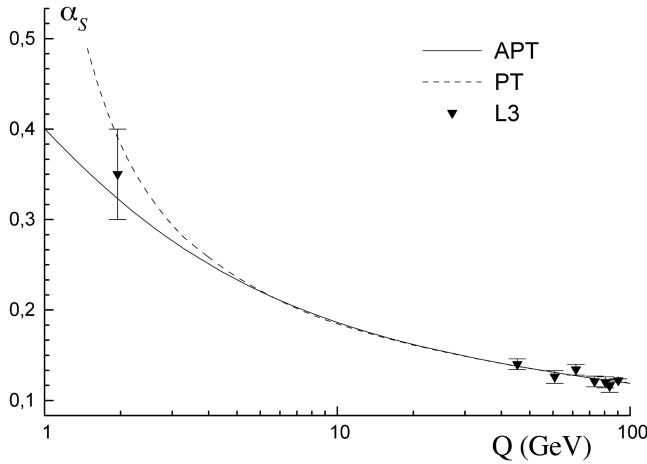


FIG. 7. QCD evolution of the running coupling constants (defined in the spacelike region) compared to experimental data.

perturbative relations; however, the PT and the APT values of  $\Lambda$  with the same number of active quarks differ by about 40%.

In Fig. 7, we plot results for the QCD evolution of  $\alpha_s(Q)$ , comparing the APT running coupling constant as discussed above which uses  $s$ -channel matching according to Eq. (26) with the standard PT running coupling constant [see Eq. (20)] which uses the matching procedure given by Eq. (28), starting from  $M_Z$  down to  $Q = M_\tau$ . Also shown on the graph is the experimental data measured by L3 Collaboration [18]. As experimental input we use the average value  $\alpha_s(M_Z) = 0.1207 \pm 0.0016$  from Ref. [18]. (In order to not encumber the figure we do not plot the corridor of errors.)

We should give a little explanation of how the spacelike APT running coupling was calculated. First, we calculate  $\Lambda_5$  from the measured value of  $\bar{\alpha}_s^{\text{APT}}(M_Z) = 0.1207$ . Then, we use this value of  $\Lambda_5$  to determine  $\bar{\alpha}_s^{\text{APT}}$  for all  $s$ , and hence through the matching procedure, determine  $\Lambda_6, \Lambda_4, \Lambda_3$ . The spectral density that we used above at  $n_f = 3$  is determined for arbitrary  $n_f$  by  $\bar{\alpha}_s^{\text{APT}}$  through  $(1/\pi)\varrho(s, \Lambda_{n_f}, n_f) = -s d\bar{\alpha}_s(s, \Lambda_{n_f}, n_f)/ds$ . An explicit formula for  $\varrho$  as a function of  $s$ ,  $\Lambda$ , and  $n_f$  is given in Eq. (24) of Ref. [12]. Then, from the spectral representation (24), we find the spacelike running coupling constant from

$$\begin{aligned} \bar{\alpha}_s^{\text{APT}}(Q) = & 4 \left[ \int_0^{4M_c^2} \frac{ds}{s+Q^2} \varrho(s, \Lambda_3, 3) \right. \\ & + \int_{4M_c^2}^{4M_b^2} \frac{ds}{s+Q^2} \varrho(s, \Lambda_4, 4) \\ & + \int_{4M_b^2}^{4M_t^2} \frac{ds}{s+Q^2} \varrho(s, \Lambda_5, 5) \\ & \left. + \int_{4M_t^2}^{\infty} \frac{ds}{s+Q^2} \varrho(s, \Lambda_6, 6) \right]. \end{aligned} \quad (29)$$

It should be stressed that in Fig. 7 we have plotted the value of the QCD running coupling constant extracted by using the perturbative parametrization. However, this is not really self-

consistent. For instance, in the case of the semileptonic decay of the  $\tau$ -lepton, to parametrize the process in the term of the QCD scale parameter  $\Lambda$  one usually uses the analytic properties of the running coupling, which are obviously broken by the perturbative approximation due to the unphysical singularities. Within the APT approach it is possible to maintain the required analytic properties and give a self-consistent description of the process [12]. That, in principle, changes the value of the QCD running coupling extracted from the experimental data. Thus, the experimental points, plotted in Fig. 7 should be considered as illustrative only. Nevertheless, it is clear that if we use a normalization point with a large value of momentum, the curve of the running coupling constant corresponding to the APT method lies below than the corresponding PT line, which, from the point of view of the perturbative description, corresponds to a smaller value of  $\Lambda$  at low energy. The fact that low energy data prefer small values of the scale parameter  $\Lambda$  and that at the same time the high energy data prefer larger values of  $\Lambda$  has been emphasized in Ref. [19]. Thus, this apparent discrepancy may be understood in the framework of the APT method; however, we should mention again that one needs to perform a reanalysis of the low energy experimental data by using the APT parametrization, as in the case of  $\tau$  decay [12], in order to extract the QCD running coupling constant.

## VIII. CONCLUSIONS

Let us briefly summarize our considerations. To determine the running coupling constant in the timelike region, we took advantage of APT because it provides a consistent procedure necessary for analytic continuation. It is to be noted that the APT method ensures not only correct analytic properties of the running coupling constant but also stability with respect to higher loop corrections, which is essential for the stability of our procedure of analytic continuation. This stability is provided, in part, by the universal infrared limit value of the running coupling constant at  $q^2 = -Q^2 \rightarrow -0$  that is invariant with respect to higher loop corrections. The proposed method of constructing the running coupling constant in the timelike region results in a function with the same universal infrared limit value when  $q^2 \rightarrow +0$ .

Quantitatively, our analysis shows that the effect of analytic continuation can be associated with  $\pi^2$ -terms only at very large momentum transfers of the order of the  $Z$ -boson mass where the contribution of the  $\pi^2$ -terms is small. At intermediate and, especially, at low momentum transfers it is important to take account of the correct analytic properties of  $\alpha_s$ , which permits a consistent transition into the timelike region. The  $Q^2$ -dependence of  $\alpha_s$  is essentially different from the dependence of  $\alpha_s$  in PT. Our analysis shows that the popular PT expressions for  $\alpha_s$  as expansions in  $1/\ln(Q^2/\Lambda^2)$ , containing nonphysical singularities, do not allow a self-consistent interpretation of information obtained from different experiments on the evolution of  $\alpha_s$  outside of the asymptotic region. From our numerical estimates it follows that analyticity of the running coupling constant has great influence on the value of the parameter  $\Lambda_{\text{QCD}}$  extracted from experimental data and on the  $Q^2$ -evolution of  $\alpha_s$ . Note that these considerations are also important for the investigation of power corrections, which are now under intensive

study (see, e.g., [20]). The importance of power corrections in the APT scheme relative to perturbative terms naturally will be different than in the conventional approach. As in PT, the influence of quark thresholds results in a reduction of the scale parameter  $\Lambda$  as the number of active flavors  $n_f$  increases. However, the importance of maintaining the correct analytic structure suggests that the required matching be made in the physical region.

The APT method appears to be fruitful for studying the problem of analytic continuation of  $\alpha_s$  into the timelike region. There is no doubt that extracting more detailed information from experimental data on timelike processes requires a more thorough theoretical analysis within APT

including the estimation of the contributions from higher order processes, mass corrections, and so on. These will be considered in our subsequent papers.

#### ACKNOWLEDGMENTS

We are grateful to D. V. Shirkov, S. V. Mikhailov, R. Ruskov, and I. L. Solovtsov for useful remarks and interest in the work. This work has been supported in part by the U.S. National Science Foundation (grant PHY-9600421) and the U.S. Department of Energy (grant DE-FG-02-95ER40923).

- 
- [1] N. N. Bogoliubov and D. V. Shirkov, *Introduction to the Theory of Quantized Fields*, 3rd ed. (Wiley, New York, 1980).
  - [2] D. V. Shirkov and I. L. Solovtsov, JINR Rap. Comm. 1996. No 2[76]-96, pp. 5–10, hep-ph/9604363; Phys. Rev. Lett. **79**, 1209 (1997).
  - [3] K. A. Milton and I. L. Solovtsov, Phys. Rev. D **55**, 5295 (1997).
  - [4] R. G. Moorhouse, M. R. Pennington, and C. G. Ross, Nucl. Phys. **B124**, 285 (1977).
  - [5] D. E. Soper and L. R. Surguladze, Phys. Rev. D **54**, 4566 (1996).
  - [6] P. A. Raczka and A. Szymacha, Phys. Rev. D **54**, 3073 (1996); P. A. Raczka, in *Tau 96*, Proceedings of the 4th Workshop on Tau Lepton Physics, Estes Park, Colorado, edited by J. Smith and W. Toki [Nucl. Phys. B (Proc. Suppl.) **55C**, 403 (1997)].
  - [7] A. V. Radyushkin, JINR Rap. Comm. 1996. No 4[78]-96, pp. 9-14; Report No. JINR, 1982, No E2-82-159.
  - [8] H. F. Jones and I. L. Solovtsov, Phys. Lett. B **349**, 519 (1995).
  - [9] R. Shankar, Phys. Rev. D **15**, 755 (1977).
  - [10] A. A. Pivovarov, Nuovo Cimento A **105**, 813 (1992).
  - [11] O. P. Solovtsova, JETP Lett. **64**, 714 (1996).
  - [12] K. A. Milton, I. L. Solovtsov, and O. P. Solovtsova, Phys. Lett. B **415**, 104 (1997).
  - [13] M. Schmelling, in *ICHEP 96*, Proceedings of the XXVIII International Conference on High Energy Physics, Warsaw, Poland, 1996, edited by Z. Ajduk and A. Wroblewski (World Scientific, Singapore, 1997), hep-ex/9701002.
  - [14] A. Pich, in *Tau 96* [6], p. 3, hep-ph/9612308; talk given at the 20th Johns Hopkins Workshop on Current Problems in Particle Theory, Heidelberg, 1996, hep-ph/97101305.
  - [15] S. G. Gorishny, A. L. Kataev, and S. A. Larin, Nuovo Cimento A **92**, 119 (1986).
  - [16] Particle Data Group, R. M. Barnett *et al.*, Phys. Rev. D **54**, 1 (1996), p. 77.
  - [17] W. J. Marciano, Phys. Rev. D **29**, 580 (1984).
  - [18] L3 Collaboration, M. Acciarri *et al.*, Phys. Lett. B **404**, 390 (1997); **411**, 339 (1997).
  - [19] M. Shifman, Int. J. Mod. Phys. A **11**, 3195 (1996).
  - [20] G. Grunberg, talk given at 32nd Rencontre de Moriond: QCD and High Energy Hadronic Interactions, Les Arcs, France, 1997, hep-ph/9705290.